A Symbiotic Plant Peroxidase Involved in Bacterial Invasion of the Tropical Legume *Sesbania rostrata*[1][C][W][OA]

Jeroen Den Herder[2], Sam Lievens[2,3], Stephane Rombauts, Marcelle Holsters*, and Sofie Goormachtig

Department of Plant Systems Biology, Flanders Institute for Biotechnology, and Department of Molecular Genetics, Ghent University, B–9052 Ghent, Belgium

Aquatic nodulation on the tropical legume *Sesbania rostrata* occurs at lateral root bases via intercellular crack-entry invasion. A gene was identified (*Srprx1*) that is transiently up-regulated during the nodulation process and codes for a functional class III plant peroxidase. The expression strictly depended on bacterial nodulation factors (NFs) and could be modulated by hydrogen peroxide, a downstream signal for crack-entry invasion. Expression was not induced after wounding or pathogen attack, indicating that the peroxidase is a symbiosis-specific isoform. In situ hybridization showed *Srprx1* transcripts around bacterial infection pockets and infection threads until they reached the central tissue of the nodule. A root nodule extensin (*SrRNE1*) colocalized with *Srprx1* both in time and space and had the same NF requirement, suggesting a function in a similar process. Finally, in mixed inoculation nodules that were invaded by NF-deficient bacteria and differed in infection thread progression, infection-associated peroxidase transcripts were not observed. Lack of *Srprx1* gene expression could be one of the causes for the aberrant structure of the infection threads.

The interaction of rhizobia with plants of the legume family results in the formation of new root structures, the nodules, in which the bacteria fix atmospheric nitrogen for assimilation by the host. A complex signal exchange between the macrosymbiont and the microsymbiont initiates the nodulation process: Upon perception of flavonoids exuded by host roots, rhizobia switch on their nodulation genes, thus forming lipochitooligosaccharide molecules, designated nodulation factors (NFs; D'Haeze and Holsters, 2002). NFs are essential for bacterial invasion and induction of cortical cell division to form nodule organs (Geurts and Bisseling, 2002).

In the model legumes *Medicago truncatula* and *Lotus japonicus*, nodulation starts with entrapment of the bacteria in a curled root hair, followed by the formation of an infection thread (IT) that grows toward the nodule primordium and from which bacteria are released and differentiate into N_2-fixing bacteroids (Gage, 2004). ITs are tubular structures that develop after membrane invagination and further extend inward by polar growth mechanisms (Gage and Margolin, 2000; Gage, 2004). How ITs can grow against the turgor of the plant cells is still unknown, but hydrogen peroxide (H_2O_2)-driven cross-linking of root nodule extensins (RNEs) might be involved (Brewin, 2004; Gucciardo et al., 2005).

An alternative route for infection occurs as an adaptation to waterlogging and has been studied in the tropical legume *Sesbania rostrata* (Goormachtig et al., 2004a). Bacteria enter the plant tissue via cracks in the epidermis at places where lateral roots have emerged from the main root or where adventitious root primordia protrude on the stem. Intercellular bacterial microcolonies or infection pockets (IPs) are created in the outer cortex, from where ITs guide the bacteria toward the nodule primordium (Den Herder et al., 2006). However, when *S. rostrata* roots are grown under aerated conditions, invasion switches from intercellular crack-entry or lateral root base (LRB) invasion to the intracellular root hair curling (RHC) mode (Goormachtig et al., 2004b).

Oxidative burst-like phenomena have been observed as a primary response of the plant both in RHC invasion and LRB entry. Early in the interaction of *Sinorhizobium meliloti* with alfalfa (*Medicago sativa*), superoxide and H_2O_2 are produced (Santos et al., 2001). In *M. truncatula* roots, recognition of compatible NFs rapidly stimulates localized production of superoxide. This response is absent in the non-nodulating plant mutant *does not make infections1-1* (*dmi1-1*), which is impaired in the NF signal transduction pathway

[1] This work was supported by the Interuniversity Poles of Attraction Programme-Belgian Science Policy (P5/13) and the Research Foundation-Flanders (grant nos. G.0066.07 and G.0341.04, predoctoral fellowships to J.D.H. and S.L., and postdoctoral fellowship to S.G.).

[2] These authors contributed equally to the article.

[3] Present address: Department of Medical Protein Research, Flanders Institute for Biotechnology, Ghent University, Albert Baertsoenkaai 3, B–9000 Ghent, Belgium.

* Corresponding author; e-mail marcelle.holsters@psb.ugent.be; fax 32–9–3313809.

The authors responsible for distribution of materials integral to the findings presented in this article in accordance with the policy described in the Instructions for Authors (www.plantphysiol.org) are: Marcelle Holsters (marcelle.holsters@psb.ugent.be) and Sofie Goormachtig (sofie.goormachtig@psb.ugent.be).

[C] Some figures in this article are displayed in color online but in black and white in the print edition.

[W] The online version of this article contains Web-only data.

[OA] Open Access articles can be viewed online without a subscription.

www.plantphysiol.org/cgi/doi/10.1104/pp.107.098764

(Ramu et al., 2002). Furthermore, H_2O_2 is found in plant cells near bacterial IPs, as well as in the matrix and walls of ITs during crack-entry invasion of *S. rostrata*. Pharmacological experiments indicate that reactive oxygen species (ROS) are required for LRB nodulation in *S. rostrata* (D'Haeze et al., 2003).

Symbiotic bacteria overcome the plant's defense by activating antioxidant enzymes (Hérouart et al., 1996; Santos et al., 1999, 2000; Sigaud et al., 1999; Jamet et al., 2003). Also, several plant genes related to protection against or production of ROS are differentially expressed during nodulation. In alfalfa roots, the enzymatic activities of catalase, ascorbate peroxidase, and glutathione reductase significantly increase upon inoculation with wild-type *S. meliloti* (Bueno et al., 2001). Moreover, a cytosolic Cu/Zn- and mitochondrial Mn-superoxide dismutase have distinct expression patterns in root nodules, suggesting specific roles for these enzymes in nodule development (Rubio et al., 2004). Finally, transcripts of a *Rhizobium*-induced peroxidase (Rip1) identified in *M. truncatula* (Cook et al., 1995) have a tissue-specific localization pattern similar to that of ROS and accumulate upon addition of exogenous H_2O_2 (Ramu et al., 2002).

Heme-binding peroxidases (Dawson, 1988) are widely distributed throughout bacteria, fungi, plants, and vertebrates and can oxidize various substrates via the reduction of H_2O_2 (Dunford and Stillman, 1976). Plant peroxidases belong to a superfamily that comprises class I intracellular peroxidases of bacterial origin, secreted fungal class II peroxidases, and classical class III secretory plant peroxidases (EC 1.11.1.7). Genes encoding the latter have been duplicated many times during evolution since their appearance in the first land plants (Duroux and Welinder, 2003; Passardi et al., 2004a). Peroxidase activity can be detected throughout the whole lifespan of a plant: from germination of the seed until the final stage of senescence and death. The lack of substrate specificity, the high number of paralogous genes, and the ability to work in two catalytic cycles account for the large variety of biological mechanisms in which plant peroxidases are involved. The enzymes have been implicated in several functions of potential importance in plant defense, including direct toxicity against pathogens, production of phytoalexins, cellular growth and cell wall loosening, auxin catabolism, and plant cell wall strengthening through different mechanisms, such as lignification, suberization, and cross-linking of cell wall proteins or phenolics (for review, see Hiraga et al., 2001; Passardi et al., 2004b, 2005).

We identified a functional class III peroxidase isoform up-regulated during nodulation of *S. rostrata* (Srprx1). Expression is transiently induced, requires bacterial NFs, and is affected by H_2O_2. Transcripts accumulate along the bacterial invasion track until the ITs reach the nodule primordium and colocalize with a RNE homolog. Furthermore, in nodules occupied by NF-deficient bacteria, peroxidase transcript levels are not induced and IT progression is hampered.

RESULTS

Srprx1 Encodes a Functional Peroxidase

Differential display was used to compare gene expression in noninoculated roots and in inoculated adventitious root primordia of *S. rostrata* at different time points (Goormachtig et al., 1995; Lievens et al., 2001). A partial 185-bp cDNA clone with homology to peroxidases was up-regulated and isolated for further characterization. The full-length clone, obtained by RACE, was designated *Srprx1* (see "Materials and Methods"). Database reference searches using the BLASTX algorithm (Altschul et al., 1997) revealed an open reading frame with high homology to plant peroxidases (Fig. 1A). Srprx1 is 70% similar to rice (*Oryza sativa*) peroxidase 131 (Passardi et al., 2004a), 70% to cationic peroxidase PNPC1 of peanut (*Arachis hypogeae*; Buffard et al., 1990), and 72% to Rip1 peroxidase of *M. truncatula* (Peng et al., 1996).

An N-terminal signal peptide for extracellular targeting was predicted at Ser-25 and the predicted mature protein displayed typical class III peroxidase features: a distal His (His-67) serving as a catalyst in the reaction with H_2O_2, a proximal His residue (His-195) involved in heme binding, and eight Cys forming four disulfide bridges (Cys-36-Cys-116, Cys-69-Cys-74, Cys-123-Cys-315, and Cys-22-Cys-227; Welinder, 1992; Fig. 1A). No potential *N*-glycosylation sites were predicted based on the known glycosylation signature Asn x (Ser-Thr) x (where x is any amino acid, except Pro; Creighton, 1993). The molecular mass of the protein without the signal peptide was estimated at 32.5 kD and the pI at 4.96, indicating that Srprx1 is an anionic peroxidase.

To demonstrate peroxidase activity, embryonic axes of *S. rostrata* were infected with an *Agrobacterium rhizogenes* strain carrying a binary vector that contained a *p35S:Srprx1* construct for constitutive *Srprx1* expression. Protein extracts from transgenic Srprx1-overproducing and control roots were subjected to native PAGE followed by in-gel 3,3′-diaminobenzidine tetrahydrochloride (DAB) staining for peroxidase activity (see "Materials and Methods"). In each sample, several brown-colored bands corresponding to DAB-oxidizing active proteins were seen. One band was much more pronounced in the overproducing than in the control extracts (Fig. 2A). In roots harvested 2 d post inoculation (dpi) with *Azorhizobium caulinodans*, this band was also more intense than in the control roots (see below; Fig. 2A). These observations indicate that the band presumably corresponds to Srprx1 and that the native protein is able to oxidize DAB in the presence of H_2O_2. In addition, blotting of the native gel immediately followed by detection with luminol showed a band in the overproduction but not in the control extracts, indicating that Srprx1 could carry out H_2O_2-dependent oxidation of several substrates (Fig. 2B).

Srprx1 Belongs to a Group of Peroxidases That Is Specific for Legumes

To search for possible orthologs, phylogenetic analysis was performed with all known and predicted

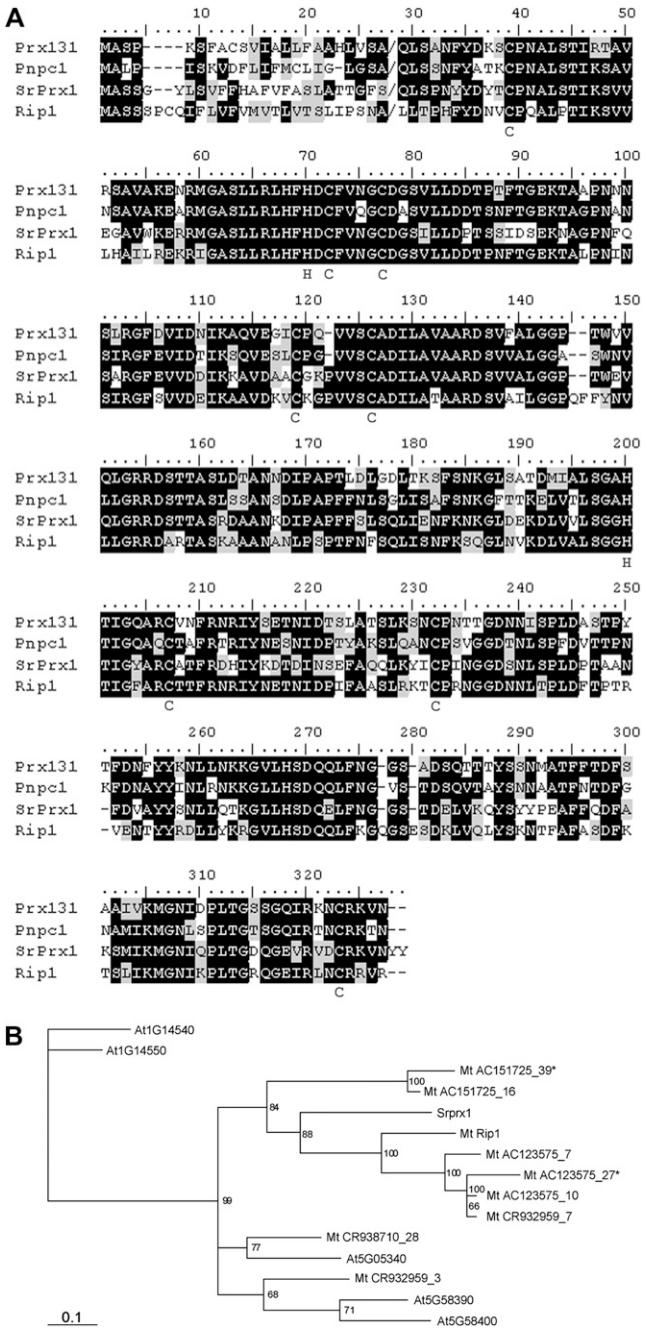

Figure 1. Srprx1 and related peroxidases. A, Alignment of Srprx1 to rice peroxidase 131 (Prx131), PNPC1 of peanut, and Rip1 of *M. truncatula*. B, Phylogenetic tree of the class III plant peroxidase subgroup, including five Arabidopsis and nine *M. truncatula* members. The maximum likelihood scores of the consensus tree are indicated (Schmidt et al., 2002). Scale represents the distance between sequences calculated based on the number of mutations (branch lengths). Numbers correspond to the locus tag for Arabidopsis (At) or the bacterial artificial clone from which they were predicted for *M. truncatula* (Mt) proteins. An asterisk marks presumed nonfunctional proteins because of the lack of some strictly conserved residues.

class III peroxidases of Arabidopsis (*Arabidopsis thaliana*), *M. truncatula*, and poplar (*Populus trichocarpa*). The resulting cladogram is shown in Supplemental Figure S1. Srprx1 belongs to a group of peroxidases that form a distinct cluster in which reside all members of Arabidopsis group IV proteins (Supplemental Fig. S1; Tognolli et al., 2002). Within this cluster, Srprx1 fits into a subcluster to which five Arabidopsis proteins belong, previously also termed group B (Supplemental Fig. S1; Duroux and Welinder, 2003). The Arabidopsis and *Medicago* proteins of the latter group were selected to repeat the phylogenetic analysis (Fig. 1B). Interestingly, Srprx1 and MtRip1 cluster together in a clade to which no Arabidopsis peroxidases belong, but that contains six other *M. truncatula* peroxidases (Fig. 1B). This observation might indicate that several peroxidases in *Medicago* have evolved to exert a specialized function, for instance, during the nodulation process.

Srprx1 Is Transiently Induced during Nodule Development

Expression of *Srprx1* was studied by semiquantitative reverse transcription (RT)-PCR analysis. RNA was prepared from uninoculated adventitious root primordia and from developing adventitious root nodules at 4, 8, and 12 h and 1, 2, 3, 4, 5, 7, 12, and 20 dpi with *A. caulinodans*. A faint signal was observed in the uninoculated sample (Fig. 3A). Transcript accumulation started approximately 12 h after inoculation and expression was maximal from 1 to 5 d. The signal decreased to low basal levels in mature 20-d-old nodules. *Srprx1* expression analysis during LRB nodulation on hydroponic roots demonstrated similar, transient induction (Fig. 3B). The uninoculated sample had a weak basal expression level and induction appeared after 30 min of inoculation to reach a maximum after 12 h. At later stages of root nodulation, the *Srprx1* transcript level decreased. When growing plants in vermiculite, thus favoring RHC invasion, similar transient induction was observed (Fig. 3B). Developing zone I root hairs had basal expression and transcript level increased after root hair colonization to reach a maximum in developing RHC nodules. In mature nodules, transcripts dropped to the basal level. Peroxidase gene expression was not detectable by RNA gel-blot hybridization in other plant tissues, including seedlings, vegetative shoot apices, flowers, and leaves. Hence, *Srprx1* expression is very specific for the early stages of developing nodules (data not shown).

Protein accumulation was investigated by gel blotting of total protein extracts of uninoculated adventitious root primordia and upon inoculation with *A. caulinodans*. An antibody was raised by rabbit injection of a 12-mer peptide sequence from Srprx1 coupled to a carrier protein (see "Materials and Methods"). Srprx1 protein accumulation was visible from 2 dpi on and reached a maximum at 5 dpi, after which it decreased slowly (Fig. 3C).

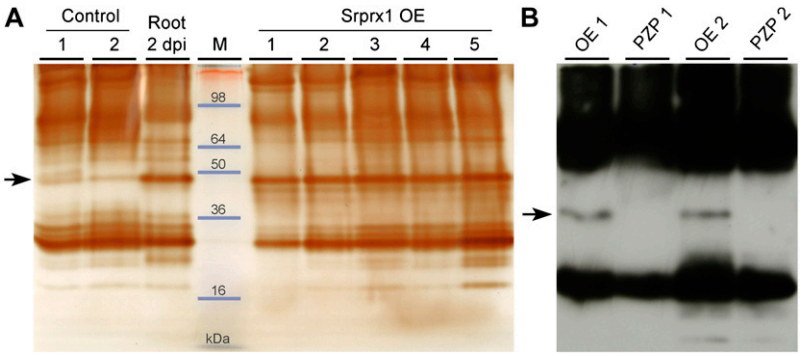

Figure 2. Srprx1 peroxidase activity. A, In-gel peroxidase activity stain. Control, Root 2 dpi, and Srprx1 OE represent protein extracts from transgenic control roots, from roots 2 dpi, and from different lines overexpressing *Srprx1*, respectively. Protein extracts were separated by native PAGE and colored with DAB in the presence of H_2O_2 for peroxidase activity. B, Chemiluminescent detection in control (PZP 1, 2) or *Srprx1*-overexpressing (OE 1, 2) plant protein extracts after native PAGE and immunoblot without secondary antibody. The Srprx1 protein is marked with an arrow. [See online article for color version of this figure.]

Srprx1 Transcripts Do Not Accumulate after Wounding or Pathogen Infection

Extracellular peroxidases are often implicated in plant responses to wounding and pathogen infection. Wound inducibility of the *Srprx1* gene was tested on leaves that were crushed with tweezers and harvested after 1, 2, 4, 8, and 16 h and 1 and 2 d. RT-PCR analysis revealed early induction of β-1,3-glucanase gene expression that served as control, indicating that strong and rapid plant reactions were triggered as a response to the mechanical damage (Fig. 4A). However, no *Srprx1* expression was detected in any of the wounded leaf samples.

To determine whether *Srprx1* transcripts accumulate in response to plant pathogens, the expression pattern was analyzed in *S. rostrata* leaves inoculated with *Botrytis cinerea*, a pathogenic fungus with a very wide host range (Staples and Mayer, 1995; Lievens et al., 2004). RNA from leaf samples harvested at different stages of the infection was subjected to RT-PCR. *Srprx1* was not induced during the plant pathogen response that was strong and early as can be deduced from β-1,3-glucanase gene expression (Fig. 4B).

In a second pathogen assay, stem-located adventitious root primordia of *S. rostrata* were infected with *Ralstonia solanacearum*, a wide host range root pathogen (Hayward, 1991) that induces a strong defense reaction at these sites (Lievens et al., 2004). Stems were brush inoculated with either the wild-type or a nonvirulent mutant strain (*hrp*$^-$) and root primordia were excised after 8 h and 1, 2, 3, and 5 d. The typical brown ring at the base of the adventitious root primordia that appeared upon wild-type *R. solanacearum* infection was accompanied at the molecular level by accumulation of β-1,3-glucanase transcripts (Fig. 3C). In this time series, RT-PCR showed no *Srprx1* induction upon pathogenesis (Fig. 4C). In conclusion, *Srprx1* expression is very specific for the early stages of developing nodules, implying that the gene encodes a nodule-specific peroxidase isoform and can be considered as one of the more specific true nodulins.

Srprx1 Expression Pattern Visualized by in Situ Hybridization

To visualize the transcripts in plant tissues, expression of *Srprx1* was analyzed by in situ hybridization on adventitious and lateral root nodule sections (Fig. 5). No expression above background was seen in sections of uninoculated adventitious root primordia (data not shown). At 1 dpi, transcripts were visible in cells neighboring the epidermal fissure that surrounds the base of the root primordium (Fig. 5, A and D). After 2 d, transcripts strongly accumulated in the cortical cells surrounding IPs (Fig. 5, B and E). At 3 dpi, ITs were formed that guide the bacteria to the nodule primordium and *Srprx1* expression was very prominent in the cells that were flanking these ITs (Fig. 5, C and F). At 4 dpi, ITs reached the nodule primordium and traversed the newly formed cells. Interestingly, *Srprx1* expression stopped abruptly once the ITs had entered the cells of the nodule primordium that would become the nodule central tissue (Fig. 5, G–I, arrows). At this stage, the signal around the fissure, the IPs, and the ITs in the outer cortex was still strong. From 6 d on, this signal gradually withdrew from the deeper cortical regions (Fig. 5J) and, at 8 d, was only faintly detectable around some remaining IPs (data not shown).

In LRBs, transcripts were visualized on butyl-methyl-embedded material in which the structure is better preserved than in paraffin (Kronenberger et al., 1993). Already at 1 dpi, *Srprx1* expression was observed at the LRBs, where the bacteria normally enter cortical tissue (data not shown). After 2 d, the lateral root was swollen at the base because of primordium development and IPs and ITs were observed. In both epidermal and cortical cells in direct contact with bacteria, transcripts accumulated (Fig. 5, K and L).

Srprx1 Expression Requires Bacterial NFs and Can Be Modulated by H_2O_2

To analyze whether *Srprx1* transcript accumulation depends on NFs, inoculations with bacterial mutants were carried out. The *A. caulinodans* strain ORS571-X15 has a Tn*5* insertion in a Rha biosynthesis locus, resulting in defective surface polysaccharides. Infection stops at the IP stage, but NF production is normal (Goethals et al., 1994; D'Haeze et al., 1998). Strain ORS571-V44 does not produce NFs because of a mutation in the *nodA* gene and is unable to provoke a nodule-related plant effect (Van den Eede et al., 1987; Mergaert et al., 1993; D'Haeze et al., 1998). *Srprx1*

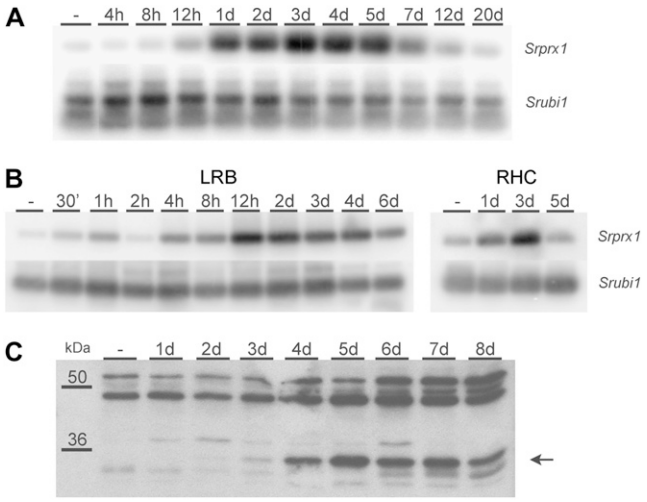

Figure 3. Expression analysis of *Srprx1* during nodule development. A, Semiquantitative RT-PCR performed on RNA from uninoculated root primordia (−) and primordia harvested at 4, 8, and 12 h and 1, 2, 3, 4, 5, 7, 12, and 20 dpi with *A. caulinodans* ORS571. B, RT-PCR on hydroponic (LRB) and aeroponic (RHC) roots after bacterial inoculation. Primers and probes specific for *Srprx1* (top) or the ubiquitin gene *Srubi1* (bottom), as a constitutive control, were used. C, Protein gel-blot of stem protein extracts before or every day after inoculation until 8 dpi. Visualization was done with primary antibody Pep2#17_63d and an anti-rabbit-IgG-HRP secondary antibody, and subsequent chemiluminescent detection. Arrow indicates Srprx1.

expression was induced by ORS571-X15, but not triggered by ORS571-V44 (Fig. 6A).

To determine whether pure *A. caulinodans* NFs are sufficient to trigger *Srprx1* transcript accumulation, roots of *S. rostrata* were treated with 10^{-8} M NFs and harvested at different time points (Fig. 6B). RT-PCR analysis showed that transcripts of the peroxidase gene already accumulated 30 min after treatment and further increased to a maximum at 12 h. Later on, the signal slowly decreased.

Because H_2O_2 is a NF downstream signal for LRB nodulation (D'Haeze et al., 2003) and induces transcription of many different genes, *Srprx1* induction was assayed by RT-PCR in hydroponic roots of *S. rostrata* supplied with 1 μm H_2O_2. Expression was slightly induced 1 h after addition and reached a maximum after 24 h, whereas thereafter it decreased again to initial levels, indicating that the expression level could be modulated by H_2O_2 (Fig. 6C).

Srprx1 Colocalizes with a RNE

In a previous differential display experiment (Goormachtig et al., 1995), a nodulation-specific tag had been isolated with homology to Hyp-rich glycoproteins with typical Ser-$(Pro)_4$ motifs. Although a full-length protein-encoding gene could not be isolated, the predicted amino acid sequence clearly displayed motifs of extensins and arabinogalactan proteins, characteristic for the group of RNEs found only in legumes (Brewin, 2004; Gucciardo et al., 2005). Also, several Tyr and isodityrosine residues (Tyr x Tyr) were present that are involved in peroxide-based protein cross-linking (Held et al., 2004; Gucciardo et al., 2005; Fig. 7A). The partial nucleotide sequence for the RNE, designated *SrRNE1*, belongs to a small gene family, as suggested by genomic DNA-blot analysis (data not shown). RT-PCR analysis showed an increase in transcript levels from 4 h after inoculation of adventitious rootlets (Fig. 7B). RNA-blot analysis after inoculation with ORS571-X15 or ORS571-V44 demonstrated that transcript accumulation depended on NF production (Fig. 7C). In situ localization of transcripts in developing adventitious root nodules revealed two major expression patterns. Two days after inoculation, transcripts accumulated around bacterial IPs and ITs (Fig. 7, E and F). At 3 dpi, expression was also visible in the nodule primordium and even more in the cells of the infection center, where ITs grew toward the open basket-shaped nodule primordium (Fig. 7, G and H). The invasion-associated pattern nicely correlated with the *Srprx1* pattern.

By using the monoclonal antibody MAC265 that is specific for RNEs in pea (*Pisum sativum*; Bradley et al.,

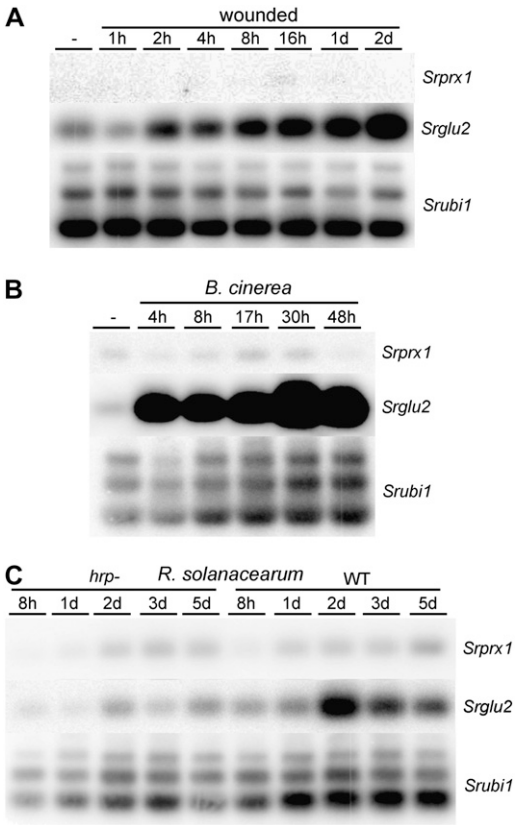

Figure 4. *Srprx1* expression in response to wounding and pathogen infection. Expression levels determined by semiquantitative RT-PCR with primers and probes specific for *Srprx1*, *Srglu2*, a β-1,3-glucanase gene as positive control, and *Srubi1* as constitutive control. A, Transcripts in leaves before (−) and 1, 2, 4, and 8 h and 1 and 2 d after wounding. B, Leaves before (−) and 4, 8, 17, 30, and 48 h after infection with a *B. cinerea* spore suspension. C, Root primordia after inoculation with either the *R. solanacearum* wild type or the avirulent *hrp*$^-$ mutant strain. Samples were taken 8 h and 1, 2, 3, and 5 dpi.

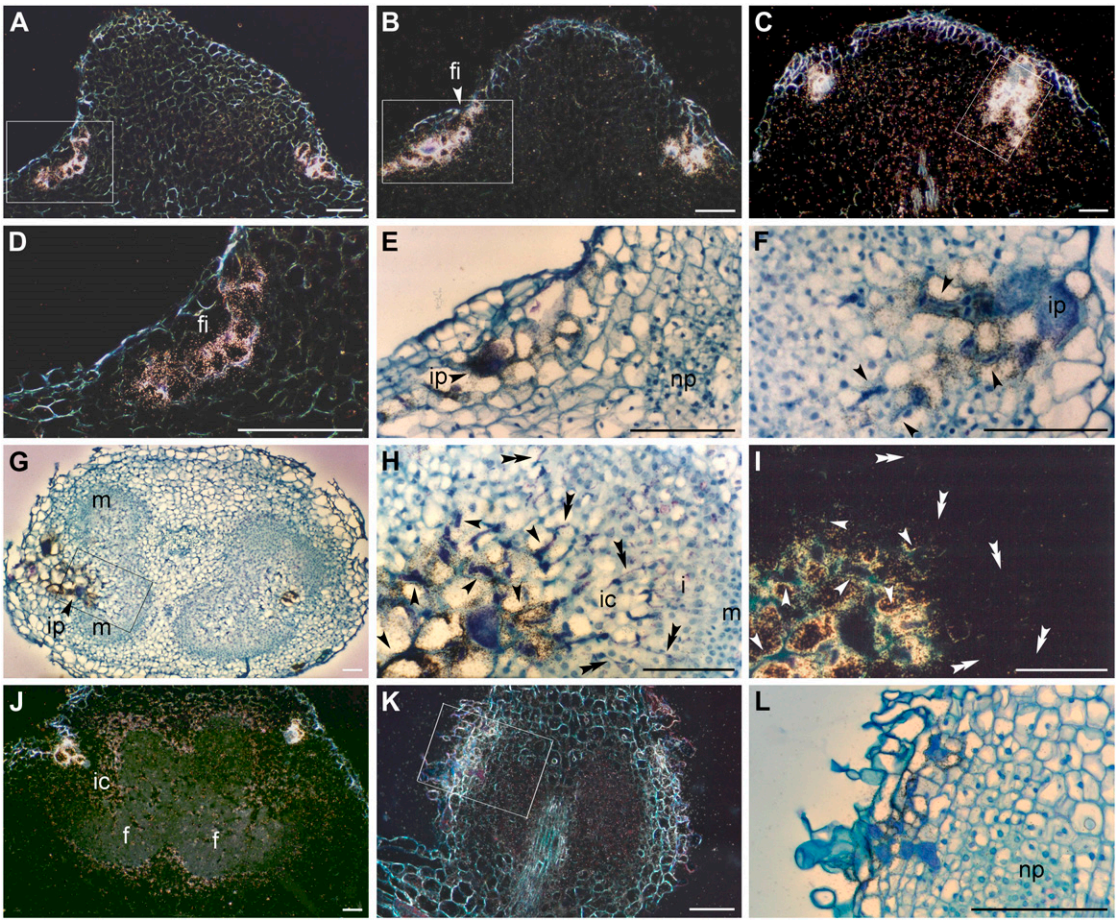

Figure 5. In situ localization of *Srprx1* transcripts. Longitudinal (A–F and J–L) and transverse (G–I) sections through developing stem (A–J) and root (K and L) nodules were hybridized with a ^{35}S-labeled antisense RNA probe and analyzed under bright-field (signal is seen as black spots [E–H and L]) and dark-field optics (signal is seen as white spots [A–D and I–K]). Successive stages of adventitious root nodule development are shown at 1 (A), 2 (B), 3 (C), 4 (G), and 6 (J) dpi with *A. caulinodans* ORS571. Images in D, E, F, H, and I are enlargements of the regions indicated by the rectangles in A, B, C, and G, respectively. K, Butyl-methyl-embedded section of a developing LRB nodule at 2 dpi. L, Enlargement of K. f, Fixation zone; fi, fissure; i, infection zone; ic, infection center; ip, infection pocket; m, meristematic zone; np, nodule primordium. Arrows and double arrows mark infection thread with or without *Srprx1* expression, respectively. Bars = 100 μm.

1988; VandenBosch et al., 1989), RNE accumulation was investigated in developing root nodules of *S. rostrata* (Fig. 7D). In uninoculated adventitious RNEs, two light bands were present around 110 and 90 kD, as similarly found in pea nodules, where immunopurified matrix glycoproteins comigrated as a doublet at 100 to 110 kD (Rathbun et al., 2002). In extracts of inoculated samples (3 dpi), these two bands were stronger and, in later stages (from 5 dpi), additional lower bands were observed, as was also the case in pea nodule extracts (Rathbun et al., 2002). Thus, RNEs accumulate in the same time frame as Srprx1 and have an overlapping expression pattern, hinting at involvement in the same biological process.

Mixed Inoculation Nodules Do Not Induce *Srprx1* Expression

Upon coinfection with two symbiotic mutants of *A. caulinodans*, ORS571-X15 and ORS571-V44, only the NF-deficient ORS571-V44 mutant invaded cortical tissue via ITs and entered plant cells to form symbiosomes (D'Haeze et al., 1998, 2004). The resulting mixed inoculation nodules developed inefficiently and bacterial invasion was not synchronized with nodule formation. Proper IT development and growth were hampered, as thick and swollen ITs were visible (Den Herder et al., 2007). During ORS571-V44 invasion, *Srprx1* was not expressed around bacterial IPs after 6 d of coinoculation, a stage that resembled early wild-type infection (Fig. 8, A and B). Only occasionally, slight induction was observed around superficial IPs, which were occupied by the NF-producing ORS571-X15 mutants (data not shown; D'Haeze et al., 1998; Den Herder et al., 2007). Around ORS571-V44-containing ITs that reached deeper into the cortical tissue after 9 d, no *Srprx1* expression was visible (Fig. 8, C and D). These observations confirm that NFs produced locally by bacteria within the ITs are required to induce the *Srprx1* gene.

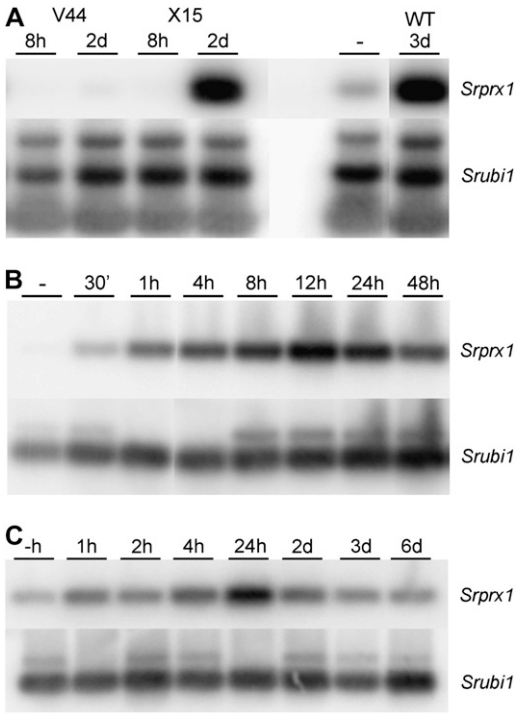

Figure 6. *Srprx1* expression in response to inoculation with *A. caulinodans* mutants, pure NFs, and H_2O_2. A, Expression after inoculation with mutants ORS571-V44 (NF deficient) and ORS571-X15 (surface polysaccharide deficient), compared to wild type as positive control. Samples were taken 8 h and 2 dpi. B, RT-PCR of *Srprx1* compared to the constitutive *Srubi1* after addition of 10^{-8} M *A. caulinodans* NFs to hydroponic roots. Samples were taken from untreated roots (−) and from roots treated for 30 min (30′) and 1, 4, 8, 12, 24, and 48 h. C, RT-PCR of *Srprx1* in hydroponic roots at different time points (−, 1, 2, 4, and 24 h, and 2, 3, and 6 d) after addition of 1 μm H_2O_2, with a constitutive control for loading (*Srubi1*).

DISCUSSION

By screening for differentially transcribed genes during adventitious root nodule development in *S. rostrata*, a short cDNA fragment was isolated, whose transcript levels increased during the early stages of infection with *A. caulinodans*. The corresponding full-length clone contained an open reading frame with high homology to class III plant peroxidases and was designated *Srprx1*.

Class III plant peroxidases (EC 1.11.1.7), often referred to as the classical plant peroxidases, are targeted to the vacuole or the extracellular space. These monomeric, usually *N*-glycosylated proteins of approximately 300 amino acids, are structurally very similar and contain four conserved disulfide bridges. The active site consists of a heme group that is coordinated to an invariant proximal His, whereas a conserved distal His is the essential catalytic residue for binding and heterolytic cleavage of H_2O_2 (Welinder, 1992). All these characteristics, with the exception of the *N*-glycosylation sites, are found in the deduced amino acid sequence of Srprx1. The presence of an N-terminal signal peptide and the absence of a vacuolar targeting sequence suggest a cell wall peroxidase. Peroxidase activity has been shown by in-gel oxidation of DAB in the presence of H_2O_2 and by luminol oxidation both in protein extracts of roots overexpressing *Srprx1* and in nodule extracts after 2 d of bacterial inoculation.

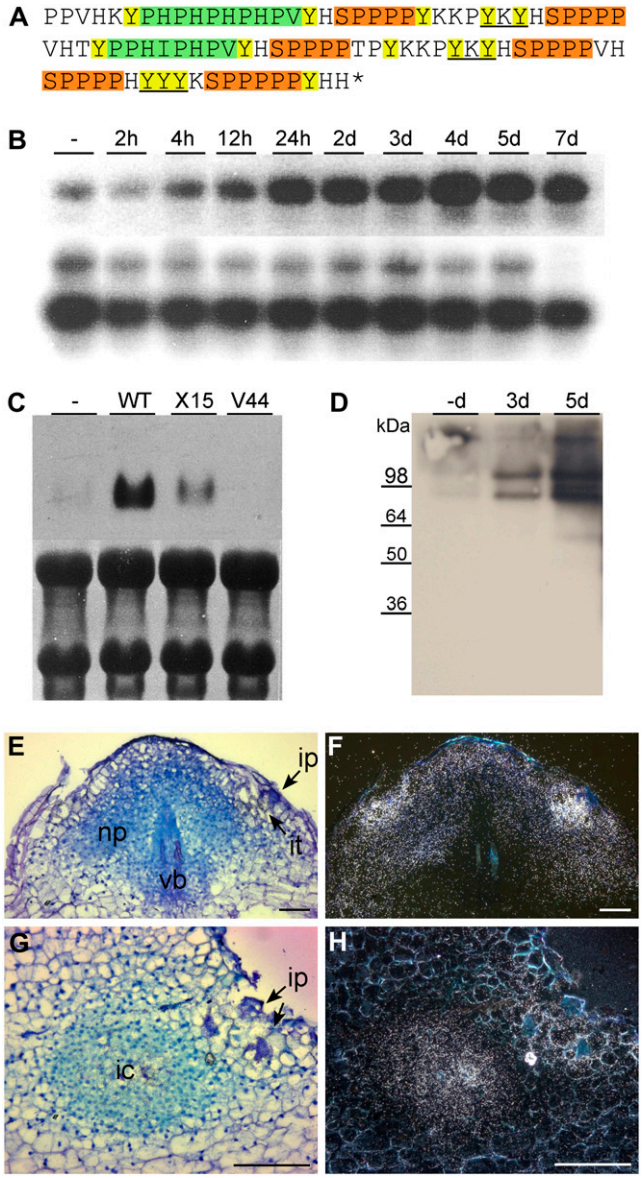

Figure 7. Analysis of *SrRNE1* during adventitious root nodule development. A, Partial protein sequence of SrRNE1 with typical extensin (orange) and arabinogalactan (green) motifs, and Tyr (yellow) and isodityrosine (underlined) residues. B, RT-PCR of *SrRNE1* (top) compared to *Srubi1* (bottom) on developing adventitious root nodules. C, RNA-blot analysis of *SrRNE1* in adventitious root primordia 3 dpi with ORS571 (WT) and mutants X15 (surface polysaccharide deficient) and V44 (NF deficient). Equal loading was controlled by methylene blue staining (bottom). D, RNE protein detection in nodule protein extracts with MAC265 antibody. E to H, In situ localization pattern of *SrRNE1* in developing adventitious root nodules at 2 (E and F) and 3 (G and H) dpi with wild-type *A. caulinodans*. ic, Infection center; ip, infection pocket; it, infection thread; np, nodule primordium; vb, vascular bundle. Bars = 100 μm.

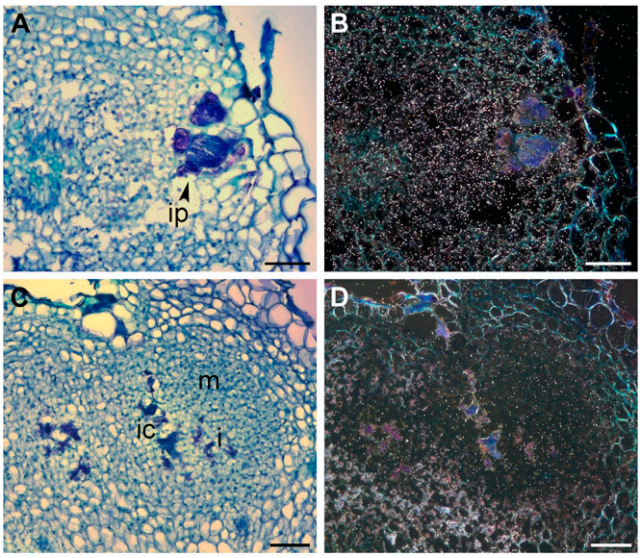

Figure 8. *Srprx1* expression in mixed inoculation nodules. In situ hybridization of *Srprx1*, 6 (A and B) and 9 (C and D) d after mixed inoculation with ORS571-V44 and ORS571-X15. i, Infection zone; ic, infection center; ip, infection pocket; m, meristematic zone. Bars = 100 μm.

Plant peroxidases are encoded by large multigene families. In the Arabidopsis genome, 73 genes have been identified, most of them expressed in roots. They account for 2.2% of root ESTs, but only a few show strict organ specificity (Tognolli et al., 2002; Welinder et al., 2002). In rice, 138 genes are distributed over all chromosomes (Passardi et al., 2004a). Also, in *S. rostrata*, *Srprx1* is part of a large family as demonstrated by DNA gel-blot analysis and activity staining of native protein extracts. Consequently, during transcript analysis, cross-hybridization with homologous family members might occur. However, with the probe used for in situ hybridization, only one gene was detected by DNA gel-blot analysis under high-stringency washing conditions (data not shown), making it unlikely that more than one family member has been visualized.

Both in adventitious and hydroponic LRB nodule development, *Srprx1* transcripts and proteins accumulated transiently during the early stages of the interaction, with a difference in time frame that corresponds to the faster nodule development on hydroponic roots. Transient induction also occurred during RHC invasion, suggesting a basic function in nodulation. *Srprx1* expression is remarkably specific for nodulation: *Srprx1* is rapidly induced by NFs, the main bacterial morphogens that control nodule development; no transcripts have been detected in other plant tissues; and the expression level did not increase upon pathogen attack, a trigger that activates various other peroxidase genes (Harrison et al., 1995; Chittoor et al., 1997; Curtis et al., 1997; Liu et al., 2005).

The temporal expression profile of *Srprx1* is somewhat reminiscent of that observed for *rip1* in *M. truncatula*. The latter gene is maximally induced in roots in the preinfection period preceding bacterial infection, but is still up-regulated after nodule primordia can be observed (96 h) to drop to basal levels afterward (Cook et al., 1995). However, in situ hybridizations indicated that *Srprx1* and *rip1* are expressed at different sites during nodule formation. The *rip1* transcripts have been localized to epidermal cells in the differentiating root zone, but also to the nascent nodule primordium (Cook et al., 1995; Peng et al., 1996). In contrast, *Srprx1* expression is tightly linked to the presence of invading rhizobia. *Srprx1* is exclusively expressed in cells that are in direct contact with NF-producing bacteria, such as those flanking the epidermal fissure, IPs, and ITs, but is restricted to the invasion preceding entry in the nodule central tissue. Thus, based on the expression data, Rip1 and Srprx1 cannot be true orthologs. Phylogenetic tree analysis indicated that Srprx1 and Rip1 cluster together in a clade that consists exclusively of *Medicago* and *Sesbania* peroxidases and that is related to the group IV peroxidases of Arabidopsis (Tognolli et al., 2002), suggesting that several peroxidases have evolved to exert a specialized function during nodule formation. The presence of seven members in *M. truncatula* points to functional redundancy or to subfunctionalization (Adams, 2007).

Class III peroxidases often use H_2O_2 as a substrate for oxidizing various biological substrates. In *S. rostrata*, H_2O_2 has been localized at the sites of *Srprx1* induction, namely, in the walls of the cells neighboring the epidermal fissure early after inoculation of root primordia, in cortical cells that will collapse to form IPs, and in intercellular and intracellular ITs (D'Haeze et al., 2003). H_2O_2 has also been shown to be a NF downstream signal for LRB invasion and to modulate *Srprx1* expression.

A putative substrate of the peroxidase could be RNEs, whose expression profile coincides with that of Srprx1. RNEs accumulate at stages similar to those of peroxidase and induction also depends on NF production. RNEs are Hyp-rich glycoproteins characterized by interspersed motifs typical for extensin and arabinogalactan proteins (Brewin, 2004; Gucciardo et al., 2005). The extensin motif with contiguous Hyp residues, such as SPPPP, is predicted to carry small Ara glycosylations, whereas clustered noncontiguous blocks of Hyp are sites for addition of large arabinogalactan polysaccharides built around a 1-3, β-linked Gal backbone (Kieliszewski, 2001; Tan et al., 2004). These matrix glycoproteins are found only in legumes and are encoded, at least in pea, by a family of genes of different length, but with very similar molecular structures (Rathbun et al., 2002).

The occurrence of a specific subgroup of Hyp-rich proteins and peroxidases in legumes and the very localized and transient induction of *Srprx1* during early nodulation stages are in agreement with a specialized role in nodulation. Peroxidative cross-linking of RNEs might have a function in the initiation of ITs

by isolating the bacteria enclosed in the curled root hair, thereby counteracting the turgor pressure of the host plant cell and driving IT growth (Brewin, 2004). A fluid-to-solid transition in the outer cortex by peroxide-driven insolubilization of RNEs might also be required during crack entry in *S. rostrata*, possibly until the ITs enter the nodule central tissue.

A functional knockout of the *Srprx1* gene might clarify these issues. Unfortunately, RNA silencing in transgenic roots yielded no nodulation phenotype (J. Den Herder, unpublished data). This outcome is not surprising because several related nodule-enhanced peroxidase gene tags have been found back in *S. rostrata* nodulation (W. Capoen and M. Holsters, unpublished data), strongly hinting at the possibility for functional redundancy. In mixed inoculation nodules that are invaded by the non-NF-producing mutant ORS571-V44 (D'Haeze et al., 1998) after initial complementation by the NF-producing, noninvasive strain ORS571-X15, *Srprx1* expression was not detected and IT progression was seriously hampered, with many bulged threads and IP-like structures in the infection center. In addition, electron microscopic analysis revealed a rim of low electron-dense material at the borders of the IT matrix that was continuous with the exopolysaccharide layer of the bacteria (Den Herder et al., 2007). The spreading of the exopolysaccharide in these ITs might be caused by changes in the physicochemical properties of the matrix. In conclusion, NF-induced functions—among them Srprx1—play a role in proper IT progression. Moreover, Srprx1 is a molecular marker that will be of great use in unraveling the components of the NF signal perception system in the cortex.

MATERIALS AND METHODS

Biological Material

Sesbania rostrata 'Brem' seeds were surface sterilized, grown, and inoculated as described (Goormachtig et al., 1995; Fernández-López et al., 1998). For root assays, plants were grown either in tubes with sterile nitrogen-free liquid Norris medium, at pH 7.0 (Vincent, 1970), or in Leonard jars with vermiculite, covered with perlite. For H_2O_2 treatment, a 30% (w/w) aqueous solution (Sigma-Aldrich) was used. Purified NFs were obtained as described (Mergaert et al., 1997) and added to a final concentration of 10^{-8} M (5×10^{-9} M of each fraction pI and pII). *Agrobacterium rhizogenes*-mediated transformation of *S. rostrata* was done as described (Van de Velde et al., 2003).

Azorhizobium caulinodans ORS571, ORS571-X15 (Goethals et al., 1994), and ORS571-V44 (Van den Eede et al., 1987) were cultivated and used for inoculation as previously described (Goormachtig et al., 1995). Infections with *Ralstonia solanacearum* and *Botrytis cinerea* were done as described by Lievens et al. (2004).

Isolation of Full-Length cDNA Clones

5′-RACE was performed with the Marathon cDNA amplification kit (CLONTECH) to obtain the full-length clone corresponding to the partial cDNA *Srdd15*. cDNA was synthesized from RNA extracted from root primordia harvested at 2 dpi with *A. caulinodans* ORS571. Antisense primer sh18 (5′-CCTGCAGTCAACACGTACTTCACCTTG-3′) in combination with the AP1 primer provided was used for the amplification step, according to the manufacturer's instructions. RACE products were cloned in the pGEM-T vector (Promega) and sequenced. The full-length sequence was designated *Srprx1*, reamplified with primers sh27 (5′-ATGGCCTCAAGCGGGTATCTCTCTG-3′) and sh28 (5′-CAATAATCTTAATTAGCTCTCAAATTTC-3′) with Vent polymerase (New England Biolabs), and cloned in the pGEM-T vector as pGEMTc6.2fl4.

For *SrRNE1*, plaques (3×10^5) of a λZAP cDNA library of developing nodules (Goormachtig et al., 1995) were screened with a ^{32}P-labeled *didi-2* fragment, an extensin-like partial cDNA isolated by differential display (Goormachtig et al., 1995). Phages from single positive plaques were transferred to their corresponding plasmid form, according to the manufacturer's protocol (Stratagene). The plasmid with the largest insert was sequenced and designated *pSrExt1*.

Protein Analysis and Activity Assay

A polyclonal antibody was raised by several rabbit injections of a 12-mer peptide sequence (LVKQYSYYPEAF) of Srprx1 with high antigenicity and low hydrophobicity (as predicted by the PeptideStructure program in the GCG Wisconsin package; Accelrys), coupled to the keyhole limpet hemocyanin protein with the Imject Maleimide Activated Immunogen conjugation kit (Pierce) via an extra Cys residue. Serum was taken 63 d after the first injection and used for protein analysis.

Plant protein extracts were prepared by grinding developing adventitious root nodules in liquid nitrogen and addition of 1 volume of extraction buffer (25 mM Tris-Cl, pH 8.0, 5 mM EDTA, 15 mM $MgCl_2$, 85 mM NaCl, 0.1% [v/v] Tween20, and protease inhibitor cocktail tablets [1/10 mL; Complete mini; Roche Diagnostics]). After 2 h of rotation at 4°C, proteins were separated from the remainder by centrifugation at 10,000*g* and 4°C for 30 min. Protein concentration of the supernatant was determined with the D_c Protein assay (Bio-Rad) and 20 μg of each sample were used for SDS-PAGE. Immunoblot was performed by blocking the membrane in 5% (w/v) skim milk in Tris-buffered saline-Tween and overnight incubation with the primary antibody (Pep2#17_63d) at 4°C (1/1,000). After washing, the secondary antibody (anti-rabbit-IgG-HRP; GE Healthcare) was incubated for 1 h at room temperature (1/10,000) and detected with a chemiluminescence kit according to the manufacturer's instructions (Perkin-Elmer). Detection of SrRNE occurred with 1% (v/v) of MAC265 hybridoma culture supernatant (Bradley et al., 1988) and anti-rat-IgG-HRP (1/10,000) as secondary antibody.

For the activity assay, extracts (prepared without Tween20) were separated on a native PAGE in Tris-Gly buffer without prior denaturation of the samples. Afterward, the gel was equilibrated for 30 min in 20 mM sodium citrate buffer (pH 5.5) before addition of 0.03% (w/v) H_2O_2 and 1 mM DAB. Replacement of the reagent mix by water stopped the reaction and the gel was dried in a gel air dryer (Bio-Rad).

RNA Analysis

RNA of roots was prepared according to Kiefer et al. (2000) and template cDNA was synthesized from 2 or 5 μg of total RNA with the SuperScript first-strand synthesis system for RT-PCR (Invitrogen). For the specific amplification of a 390-bp fragment of the 3′ end of *Srprx1*, primers sl88 (5′-TTCTGGAGGACACACGATTG-3′) and sl57 (5′-TAGTAGTTGACTTTCCTGCAGTC-3′) were used. As controls, a ubiquitin (Corich et al., 1998) and a β-1,3-glucanase (Lievens et al., 2004) fragment were amplified. Amplification of the *SrRNE1* fragment occurred with primers Ext1 (5′-CACACCTACCCTCCCCATATTCCCC-3′) and Ext2 (5′-CCCCGATCTTATAACCTTCTC-3′). The program comprised 20 cycles of amplification for 30 s at 94°C, 30 s at 60°C, and 30 s at 72°C. PCR products were detected radioactively with probes generated from the cDNA fragment *Srdd15*, *Srubi1* (Corich et al., 1998), *Srglu2* (Lievens et al., 2004), and *Srext1* by means of the Rediprime II random prime labeling system (GE Healthcare). Membranes were analyzed with a PhosphorImager (GE Healthcare). RT-PCR analysis was repeated at least twice with independent material.

RNA blot was performed by separation of 10 μg RNA from the different tissue samples on a 1% (w/v) agarose gel containing 2% (w/v) formaldehyde, transfer to Hybond-N filters (GE Healthcare), and hybridization with the corresponding *didi-2* fragment. As a control for equal loading, filters were stained with methylene blue (Sambrook et al., 1989).

In Situ Hybridization

Sections of paraffin-embedded (10 μm) or butyl-methyl-embedded (8 μm) root primordia and developing adventitious root nodules were hybridized in situ as described by Goormachtig et al. (1997). The plasmid pGEMTc6.2fl4 was digested with *Sac*II and *Sac*I to yield templates for ^{35}S-labeled antisense and

sense probe production with SP6 and T7 RNA polymerase (GE Healthcare), respectively. For *SrRNE1*, sense and antisense probes were generated by digestion of pSrExt1 with *Xho*I or *Eco*RI and transcription with T7 and T3 RNA polymerase, respectively (Goormachtig et al., 1995). Hybridizations with the sense probe did not yield signal above background (data not shown).

Phylogenetic Analysis

All potential peroxidases were collected by running reciprocal best hits iteratively with BLASTP over different proteomes, namely, poplar (*Populus trichocarpa*; Joint Genome Institute), *Medicago* (International Medicago Genome Annotation Group), and Arabidopsis (*Arabidopsis thaliana*; The Arabidopsis Information Resource) starting with the *S. rostrata* gene. From the nonredundant set of 275 proteins collected over the three genomes (137, 64, and 57 proteins, respectively), a guide tree was made on the most conserved regions in the alignment. Based on this cladogram, a proper phylogenetic tree was built for a subset of proteins with the Tree-puzzle program (Schmidt et al., 2002) to calculate a neighbor-joining tree with puzzling steps.

Sequence Analysis

DNA sequencing was carried out with universal SP6 and T7 primers. DNA sequence data were assembled and analyzed with the GCG package (Accelrys). Percentage of identity and similarity between sequences was determined with the GAP program and aligned with the PileUp program. The Srprx1 protein sequence was deduced with the Translate program and further analysis was done with the programs SPScan, Motifs, PeptideSort, and Isoelectric (all from the GCG package).

Sequence data from this article can be found in the GenBank/EMBL data libraries under accession numbers EF055261 and Z48673.

Supplemental Data

The following materials are available in the online version of this article.

Supplemental Figure S1. Cladogram of Srprx1 constructed with known and predicted class III plant peroxidases of Arabidopsis, *M. truncatula*, and poplar.

ACKNOWLEDGMENTS

We thank Monica Höfte and Frédérique Van Gijsegem for the kind gift of the *B. cinerea* spores and *R. solanacearum* strains, respectively; Nick Brewin for providing the MAC265 antibody; Annick De Keyser and Christa Verplancke for technical help; Wilson Ardiles for sequencing; and Martine De Cock for help in preparing the manuscript.

Received March 1, 2007; accepted March 22, 2007; published March 23, 2007.

LITERATURE CITED

Adams KL (2007) Evolution of duplicate gene expression in polyploid and hybrid plants. J Hered (in press)

Altschul SF, Madden TL, Schäffer AA, Zhang J, Zhang Z, Miller W, Lipman DJ (1997) Gapped BLAST and PSI-BLAST: a new generation of protein database search programs. Nucleic Acids Res **25:** 3389–3402

Bradley DJ, Wood EA, Larkins AP, Galfre G, Butcher GW, Brewin NJ (1988) Isolation of monoclonal antibodies reacting with peribacteroid membranes and other components of pea root nodules containing *Rhizobium leguminosarum*. Planta **173:** 149–160

Brewin NJ (2004) Plant cell wall remodelling in the Rhizobium—legume symbiosis. CRC Crit Rev Plant Sci **23:** 293–316

Bueno P, Soto MJ, Rodríguez-Rosales MP, Sanjuan J, Olivares J, Donaire JP (2001) Time-course of lipoxygenase, antioxidant enzyme activities and H_2O_2 accumulation during the early stages of *Rhizobium*-legume symbiosis. New Phytol **152:** 91–96

Buffard D, Breda C, van Huystee RB, Asemota O, Pierre M, Dang Ha DB, Esnault R (1990) Molecular cloning of complementary DNAs encoding two cationic peroxidases from cultivated peanut cells. Proc Natl Acad Sci USA **87:** 8874–8878

Chittoor JM, Leach JE, White FF (1997) Differential induction of a peroxidase gene family during infection of rice by *Xanthomonas oryzae* pv. *oryzae*. Mol Plant-Microbe Interact **10:** 861–871

Cook D, Dreyer D, Bonnet D, Howell M, Nony E, VandenBosch K (1995) Transient induction of a peroxidase gene in *Medicago truncatula* precedes infection by *Rhizobium meliloti*. Plant Cell **7:** 43–55

Corich V, Goormachtig S, Lievens S, Van Montagu M, Holsters M (1998) Patterns of *ENOD40* gene expression in stem-borne nodules of *Sesbania rostrata*. Plant Mol Biol **37:** 67–76

Creighton TE (1993) Proteins, Structures and Molecular Properties, Ed 2. W.H. Freeman and Company, New York

Curtis MD, Rae AL, Rusu AG, Harrison SJ, Manners JM (1997) A peroxidase gene promoter induced by phytopathogens and methyl jasmonate in transgenic plants. Mol Plant-Microbe Interact **10:** 326–338

D'Haeze W, De Rycke R, Mathis R, Goormachtig S, Pagnotta S, Verplancke C, Capoen W, Holsters M (2003) Reactive oxygen species and ethylene play a positive role in lateral root base nodulation of a semiaquatic legume. Proc Natl Acad Sci USA **100:** 11789–11794

D'Haeze W, Gao M, De Rycke R, Van Montagu M, Engler G, Holsters M (1998) Roles for azorhizobial Nod factors and surface polysaccharides in intercellular invasion and nodule penetration, respectively. Mol Plant-Microbe Interact **11:** 999–1008

D'Haeze W, Glushka J, De Rycke R, Holsters M, Carlson RW (2004) Structural characterization of extracellular polysaccharides of *Azorhizobium caulinodans* and importance for nodule initiation on *Sesbania rostrata*. Mol Microbiol **52:** 485–500

D'Haeze W, Holsters M (2002) Nod factor structures, responses, and perception during initiation of nodule development. Glycobiology **12:** 79R–105R

Dawson JH (1988) Probing structure-function relations in heme-containing oxygenases and peroxidases. Science **240:** 433–439

Den Herder G, Schroeyers K, Holsters M, Goormachtig S (2006) Signaling and gene expression for water-tolerant legume nodulation. CRC Crit Rev Plant Sci **25:** 367–380

Den Herder J, Vanhee C, De Rycke R, Corich V, Holsters M, Goormachtig S (2007) Nod factor perception during infection thread growth fine-tunes nodulation. Mol Plant-Microbe Interact **20:** 129–137

Dunford HB, Stillman JS (1976) On the function and mechanism of action of peroxidases. Coord Chem Rev **19:** 187–251

Duroux L, Welinder KG (2003) The peroxidase gene family in plants: a phylogenetic overview. J Mol Evol **57:** 397–407

Fernández-López M, Goormachtig S, Gao M, D'Haeze W, Van Montagu M, Holsters M (1998) Ethylene-mediated phenotypic plasticity in root nodule development on *Sesbania rostrata*. Proc Natl Acad Sci USA **95:** 12724–12728

Gage DJ (2004) Infection and invasion of roots by symbiotic, nitrogen-fixing rhizobia during nodulation of temperate legumes. Microbiol Mol Biol Rev **68:** 280–300

Gage DJ, Margolin W (2000) Hanging by a thread: invasion of legume plants by rhizobia. Curr Opin Microbiol **3:** 613–617

Geurts R, Bisseling T (2002) *Rhizobium* Nod factor perception and signaling. Plant Cell (Suppl) **14:** S239–S249

Goethals K, Leyman B, Van den Eede G, Van Montagu M, Holsters M (1994) An *Azorhizobium caulinodans* ORS571 locus involved in lipopolysaccharide production and nodule formation on *Sesbania rostrata* stems and roots. J Bacteriol **176:** 92–99

Goormachtig S, Alves-Ferreira M, Van Montagu M, Engler G, Holsters M (1997) Expression of cell cycle genes during *Sesbania rostrata* stem nodule development. Mol Plant-Microbe Interact **10:** 316–325

Goormachtig S, Capoen W, James EK, Holsters M (2004a) Switch from intracellular to intercellular invasion during water stress-tolerant legume nodulation. Proc Natl Acad Sci USA **101:** 6303–6308

Goormachtig S, Capoen W, Holsters M (2004b) *Rhizobium* infection: lessons from the versatile nodulation behaviour of water-tolerant legumes. Trends Plant Sci **9:** 518–522

Goormachtig S, Valerio-Lepiniec M, Szczyglowski K, Van Montagu M, Holsters M, de Bruijn FJ (1995) Use of differential display to identify novel *Sesbania rostrata* genes enhanced by *Azorhizobium caulinodans* infection. Mol Plant-Microbe Interact **8:** 816–824

Gucciardo S, Rathbun EA, Shanks M, Jenkyns S, Mak L, Durrant MC, Brewin NJ (2005) Epitope tagging of legume root nodule extensin

modifies protein structure and crosslinking in cell walls of transformed tobacco leaves. Mol Plant-Microbe Interact **18:** 24–32

Harrison SJ, Curtis MD, McIntyre CL, Maclean DJ, Manners JM (1995) Differential expression of peroxidase isogenes during the early stages of infection of the tropical forage legume *Stylosanthes humilis* by *Colletotrichum gloeosporioides*. Mol Plant-Microbe Interact **8:** 398–406

Hayward AC (1991) Biology and epidemiology of bacterial wilt caused by *Pseudomonas solanacearum*. Annu Rev Phytopathol **29:** 65–87

Held MA, Tan L, Kamyab A, Hare M, Shpak E, Kieliszewski MJ (2004) Di-isodityrosine is the intermolecular cross-link of isodityrosine-rich extensin analogs cross-linked *in vitro*. J Biol Chem **279:** 55474–55482

Hérouart D, Sigaud S, Moreau S, Frendo P, Touati D, Puppo A (1996) Cloning and characterization of the *katA* gene of *Rhizobium meliloti* encoding a hydrogen peroxide-inducible catalase. J Bacteriol **178:** 6802–6809

Hiraga S, Sasaki K, Ito H, Ohashi Y, Matsui H (2001) A large family of class III plant peroxidases. Plant Cell Physiol **42:** 462–468

Jamet A, Sigaud S, Van de Sype G, Puppo A, Hérouart D (2003) Expression of the bacterial catalase genes during *Sinorhizobium meliloti-Medicago sativa* symbiosis and their crucial role during the infection process. Mol Plant-Microbe Interact **16:** 217–225

Kiefer E, Heller W, Ernst D (2000) A simple and efficient protocol for isolation of functional RNA from plant tissues rich in secondary metabolites. Plant Mol Biol Rep **18:** 33–39

Kieliszewski MJ (2001) The latest hype on Hyp-*O*-glycosylation codes. Phytochemistry **57:** 319–323

Kronenberger J, Desprez T, Höfte H, Caboche M, Traas J (1993) A methacrylate embedding procedure developed for immunolocalization on plant tissues is also compatible with in situ hybridization. Cell Biol Int **17:** 1013–1021

Lievens S, Goormachtig S, Holsters M (2001) A critical evaluation of differential display as a tool to identify genes involved in legume nodulation: looking back and looking forward. Nucleic Acids Res **17:** 3459–3468

Lievens S, Goormachtig S, Holsters M (2004) Nodule-enhanced protease inhibitor gene: emerging patterns of gene expression in nodule development on *Sesbania rostrata*. J Exp Bot **55:** 89–94

Liu G, Sheng X, Greenshields DL, Ogieglo A, Kaminskyj S, Selvaraj G, Wei Y (2005) Profiling of wheat class III peroxidase genes derived from powdery mildew-attacked epidermis reveals distinct sequence-associated expression patterns. Mol Plant-Microbe Interact **18:** 730–741

Mergaert P, Ferro M, D'Haeze W, Van Montagu M, Holsters M, Promé J-C (1997) Nod factors of *Azorhizobium caulinodans* strain ORS571 can be glycosylated with an arabinosyl group, a fucosyl group, or both. Mol Plant-Microbe Interact **10:** 683–687

Mergaert P, Van Montagu M, Promé J-C, Holsters M (1993) Three unusual modifications, a D-arabinosyl, an *N*-methyl, and a carbamoyl group, are present on the Nod factors of *Azorhizobium caulinodans* strain ORS571. Proc Natl Acad Sci USA **90:** 1551–1555

Passardi F, Cosio C, Penel C, Dunand C (2005) Peroxidases have more functions than a Swiss army knife. Plant Cell Rep **24:** 255–265

Passardi F, Longet D, Penel C, Dunand C (2004a) The class III peroxidase multigenic family in rice and its evolution in land plants. Phytochemistry **65:** 1879–1893

Passardi F, Penel C, Dunand C (2004b) Performing the paradoxical: how plant peroxidases modify the cell wall. Trends Plant Sci **9:** 534–540

Peng H-M, Dreyer DA, VandenBosch KA, Cook D (1996) Gene structure and differential regulation of the *Rhizobium*-induced peroxidase gene *rip1*. Plant Physiol **112:** 1437–1446

Ramu SK, Peng H-M, Cook DR (2002) Nod factor induction of reactive oxygen species production is correlated with expression of the early nodulin gene *rip1* in *Medicago truncatula*. Mol Plant-Microbe Interact **15:** 522–528

Rathbun EA, Naldrett MJ, Brewin NJ (2002) Identification of a family of extensin-like glycoproteins in the lumen of *Rhizobium*-induced infection threads in pea root nodules. Mol Plant-Microbe Interact **15:** 350–359

Rubio MC, James EK, Clemente MR, Bucciarelli B, Fedorova M, Vance CP, Becana M (2004) Localization of superoxide dismutases and hydrogen peroxide in legume root nodules. Mol Plant-Microbe Interact **17:** 1294–1305

Sambrook J, Fritsch EF, Maniatis T (1989) Molecular Cloning: A Laboratory Manual, Ed 2. Cold Spring Harbor Laboratory Press, Cold Spring Harbor, NY

Santos R, Bocquet S, Puppo A, Touati D (1999) Characterization of an atypical superoxide dismutase from *Sinorhizobium meliloti*. J Bacteriol **181:** 4509–4516

Santos R, Hérouart D, Puppo A, Touati D (2000) Critical protective role of bacterial superoxide dismutase in *Rhizobium*-legume symbiosis. Mol Microbiol **38:** 750–759

Santos R, Hérouart D, Sigaud S, Touati D, Puppo A (2001) Oxidative burst in alfalfa-*Sinorhizobium meliloti* symbiotic interaction. Mol Plant-Microbe Interact **14:** 86–89

Schmidt HA, Strimmer K, Vingron M, von Haeseler A (2002) TREE-PUZZLE: maximum likelihood phylogenetic analysis using quartets and parallel computing. Bioinformatics **18:** 502–504

Sigaud S, Becquet V, Frendo P, Puppo A, Hérouart D (1999) Differential regulation of two divergent *Sinorhizobium meliloti* genes for HPII-like catalases during free-living growth and protective role of both catalases during symbiosis. J Bacteriol **181:** 2634–2639

Staples RC, Mayer AM (1995) Putative virulence factors of *Botrytis cinerea* acting as a wound pathogen. FEMS Microbiol Lett **134:** 1–7

Tan L, Qiu F, Lamport DTA, Kieliszewski MJ (2004) Structure of a hydroxyproline (Hyp)-arabinogalactan polysaccharide from repetitive Ala-Hyp expressed in transgenic *Nicotiana tabacum*. J Biol Chem **279:** 13156–13165

Tognolli M, Penel C, Greppin H, Simon P (2002) Analysis and expression of the class III peroxidase large gene family in *Arabidopsis thaliana*. Gene **288:** 129–138

Van de Velde W, Mergeay J, Holsters M, Goormachtig S (2003) *Agrobacterium rhizogenes*-mediated transformation of *Sesbania rostrata*. Plant Sci **165:** 1281–1288

Van den Eede G, Dreyfus B, Goethals K, Van Montagu M, Holsters M (1987) Identification and cloning of nodulation genes from the stem-nodulating bacterium ORS571. Mol Gen Genet **206:** 291–299

VandenBosch KA, Bradley DJ, Knox JP, Perotto S, Butcher GW, Brewin NJ (1989) Common components of the infection thread matrix and the intercellular space identified by immunocytochemical analysis of pea nodules and uninfected roots. EMBO J **8:** 335–342

Vincent JM (1970) A Manual for the Practical Study of the Root-Nodule Bacteria. IBP Handbook No. 15. Blackwell Scientific Publications, Oxford

Welinder KG (1992) Superfamily of plant, fungal and bacterial peroxidases. Curr Opin Struct Biol **2:** 388–393

Welinder KG, Justesen AF, Kjærsgård IVH, Jensen RB, Rasmussen SK, Jespersen HM, Duroux L (2002) Structural diversity and transcription of class III peroxidases from *Arabidopsis thaliana*. Eur J Biochem **269:** 6063–6081